Hindawi Publishing Corporation
Journal of Composites
Volume 2014, Article ID 769379, 9 pages
http://dx.doi.org/10.1155/2014/769379

Research Article

Mechanical and Dielectric Behaviour of $CaCu_3Ti_4O_{12}$ and Nb Doped $CaCu_3Ti_4O_{12}$ Poly(vinylidene fluoride) Composites

Anshuman Srivastava,[1] Karun Kumar Jana,[2] Pralay Maiti,[2] Devendra Kumar,[1] and Om Parkash[1]

[1]*Department of Ceramic Engineering, Indian Institute of Technology (Banaras Hindu University), Varanasi 221005, India*
[2]*School of Material Science and Technology, Indian Institute of Technology (Banaras Hindu University), Varanasi 221005, India*

Correspondence should be addressed to Om Parkash; oprakash.cer@itbhu.ac.in

Received 22 August 2014; Accepted 25 November 2014; Published 14 December 2014

Academic Editor: Masamichi Kawai

PVDF has been reinforced with different amount of $CaCu_3Ti_{4-5x/4}Nb_xO_{12}$ with $x = 0.05$ powder prepared by solid state ceramic method. Composites were prepared by melt extrusion method. Phase composition was studied using powder X-ray diffraction (XRD). Microstructural, dielectric, and mechanical properties have also been studied. These composites have Young's modulus more than that of pure PVDF. Two dielectric relaxations, one at low frequency and the other at high frequency, have been observed in these composites. Dielectric relaxation at low frequencies is of Maxwell-Wagner type while the one observed at high frequency is due to hopping of electrons among different valent states of transition metal ions. Nature of dielectric relaxation has been analysed using H-N function.

1. Introduction

Nowadays, polymer-ceramic composites have gained a lot of interest as potential candidates for many applications such as embedded capacitors, microelectronic packaging, and charge storage devices. Polymers possess good processability, mechanical flexibility and low cost but have very small value of dielectric constant to be useful as capacitors. On the other hand, ferroelectric and relaxor ferroelectric ceramics have high dielectric constant but these are brittle. Dielectric constant of these ceramics is very sensitive to temperature near their transition point. This is not a desirable feature for use of these materials as capacitors. Therefore, polymer-ceramic composites can be a good choice to achieve miniaturisation of energy storage devices by combining the merits of polymers and ceramics [1–4]. Barium titanate ($BaTiO_3$, BT), lead zirconate titanate ($Pb(Zr,Ti)O_3$, PZT), and lead magnesium niobate-lead titanate ($Pb(Mgl/3Nb2/3)O_3PbTiO_3$, PMNT-PT) have been widely used as fillers by many research groups [5–12].

$CaCu_3Ti_4O_{12}$ (CCTO) has attracted increasing scientific and technological interest. Being lead-free, it is environment-friendly possessing high dielectric constant which is nearly temperature- (T-) independent in the range 100–600 K [13, 14]. Dielectric properties of composites depend on the dielectric properties of the ceramic filler, polymer matrix, and the interfaces between the filler and the matrix [3]. At high loading, the filler particles have a tendency to agglomerate resulting in an increase in porosity, decrease in densification, low dielectric constant, poor mechanical properties, and high water absorption. These problems are further enhanced due to difference in the surface characteristics of inorganic filler and the organic matrix. Homogeneous dispersion becomes more difficult at high volume fraction of the filler.

Polymers such as epoxy, cyanate ester, polyethersulfone, and polyvinylidene fluoride (PVDF) have been used as matrices [15, 16]. Arabati et al. reported dielectric properties of CCTO reinforced PVDF composites for the first time. They studied the dielectric behaviour of multilayer stack of solution cast films packed in a sandwich configuration. A dielectric constant of value 150–260 was obtained for the composite layers based on the thickness ratio of copolymer layers to composite layers and dielectric constant of

copolymer [17]. Since then, many such composite systems containing different polymers and CCTO have been studied using different particles size of ceramic phase.

Among these polymers, ferroelectric PVDF has been widely used as a matrix material due to its pyroelectric, piezoelectric properties and thermoplastic behaviour. Effect of particle size on the dielectric properties of CCTO/PVDF composites was studied by Yang et al. [14]. For 40 vol% of CCTO, they obtained a value of $\varepsilon' > 10^6$ for nanosize CCTO and 35.7 for microsize CCTO at 10^2 Hz and at room temperature. Yang et al. studied the effect of coupling agent on the PVDF-CCTO composites using 0.1 mL of Si69 coupling agent. A value of ε', 84, for PVDF/CCTO composite was obtained; ε' value was 16 in the case of PVDF/CCTO composite without coupling agent [18]. Zhang reported a dielectric constant of 62 having a loss tangent of 0.05 for nanocomposites containing 50 vol% CCTO at room temperature and 1 KHz [19]. Thomas et al. reported an increase in the value of dielectric constant of PVDF from 18 to 87 for 30 vol% of nanocrystallites of CCTO in PVDF composite at 100 Hz [20]. Dang et al. reported a dielectric constant of value ~49 at 100 Hz and at room temperature for a composite film of CCTO/polyimide [21]. Thomas et al. reported a value of dielectric constant 95 at 100 Hz for 55 volume % of CCTO in PVDF [22]. Most of the above studies were limited to only dielectric behaviour.

It is universally accepted that modifications of composition by substitution of other ions and preparation methods have a strong influence on the dielectric properties of the ceramics. The intrinsic dielectric response in CCTO is due to internal barrier layer (IBL) formation at grain boundaries which results in interfacial polarization [23]. Permittivity also depends on the microstructure. Doping modifies the grain boundaries leading to more efficient IBLC [23]. Therefore, a high ε polymer-ceramic composite can be developed at low vol % of reinforcement and some of the problems associated with fabrication can be eliminated. Sulaiman et al. prepared CCTO electroceramic using solid state reaction method [24]. They found that CCTO doped with 1 mol% Nb gave the highest dielectric constant of 18,000 at 1 MHz. Hong et al. synthesised Nb substituted CCTO using solid state reaction method [25]. They found the value of dielectric constant around ~420000 at 10 KHz for $x = 0.2$ in the system $CaCu_3Ti_{4-x}Nb_xO_{12+\delta}$.

In the present work, CCTO and $CaCu_3Ti_{4-5x/4}Nb_xO_{12}$ with $x = 0.05$ have been synthesised by solid state technique. This ceramic was dispersed in the PVDF matrix to develop high ε composites. Mechanical properties of these composites have been studied as these are as important as dielectric properties. Earlier studies on these high ε polymer-ceramic composites lacked study of their mechanical properties.

2. Experimental

2.1. Materials. Poly(vinylidene fluoride) (PVDF) (SOLEF 6008; Ausimont, Italy), with a melt flow index of 24 g/10 min at 230°C under a 5 kg load, was used in this work. CCTO and Nb doped CCTO were prepared by conventional solid state technique. Powders of $CaCO_3$(99.98%), CuO (99.5%), TiO_2(99.55), and Nb_2O_5 (99.98%) were mixed in stoichiometric amount and ground for 8 hours. These were calcined in air at 1000°C for 12 hours with intermittent grinding. Formation of single phase solid solution was confirmed by powder X-ray diffraction (XRD) using CuKα radiation. The calcined powder was ground and mixed with 2% PVA (molecular weight 37000) solution and cold pressed into pellets having 15 mm diameter and 2 mm thickness under a load of 7 tons, using a hydraulic press. The pressed pellets were sintered at 1000°C for 6 hours. Sintered pallets were ground using an agate mortar and pestle to get a fine powder.

2.2. Composite Preparation. Melt extrusion process was used for fabrication of PVDF/NbCCTO composites. In this method, 12 gms of polymer was mixed with 10, 20, and 50 wt% of ceramic (NbCCTO) in a high speed mixer for 20 min before putting it into the extruder. Extrusion was carried out in a twin-screw extruder (Hakke Mini Lab). Mixing was done at 205°C for ~10 minutes under a speed of 70 rpm. The polymer chains mix uniformly with the ceramic particles during melt mixing. PVDF and composites were melt-pressed into thin films of 100 μm thickness in a compression-molding machine at 190°C under a load of 5 tons.

2.3. Characterization

2.3.1. X-Ray Diffraction. X-ray diffraction (XRD) patterns were recorded using a Rigaku Desktop Miniflex II X-Ray diffractometer employing Cu-Kα radiation (wavelength, λ = 0.1548 nm) and Ni-filter. Thin films of PVDF and composites were scanned in the 2θ angle range 10–90° at a 3°/min.

2.3.2. FTIR. Fourier transform infrared spectra (FTIR) of pure PVDF, pure ceramics, and composites were recorded in the range 2000 to 600 cm^{-1} using thin films. Pellets of ceramic powder were made using KBr.

2.3.3. Scanning Electron Microscope. SEM images were recorded using INSPECT S 50 FP 2017/12 scanning electron microscope. Samples were coated with gold to make the surface conducting.

2.3.4. Mechanical Properties. Tensile tests were performed on the microinjected dog bone shaped samples at room temperature using Instron 3369 tensile machine. A constant crosshead speed of 5 mm/min was selected and the stress-strain data were recorded till the samples broke. Two samples of each composition were tested.

2.3.5. Dielectric Measurements. Dielectric measurements were made on disc-shaped films having 12 mm diameter. These were silver-coated on opposite faces and measurements were made between 10^{-2} and 10^6 Hz using four-probe Novocontrol setup (ZG4) from room temperature to 120°C.

3. Results and Discussion

3.1. Structural Analysis. X-ray diffraction patterns of NbCCTO, PVDF, and their composites containing 10, 20, and

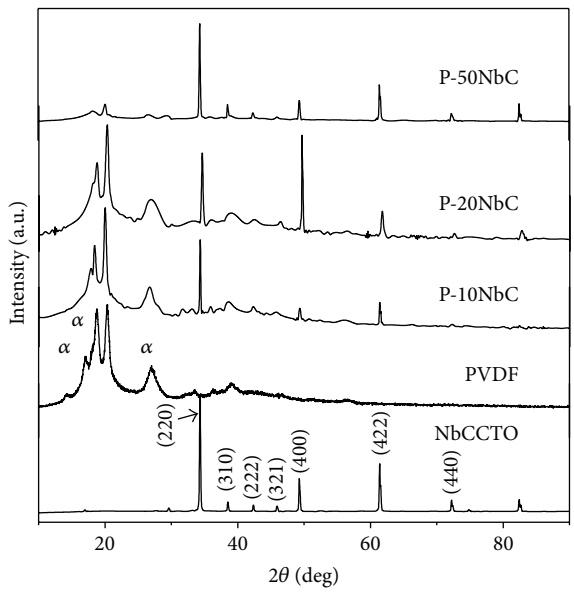

Figure 1: X-ray diffraction patterns for NbCCTO and pure PVDF and its composites.

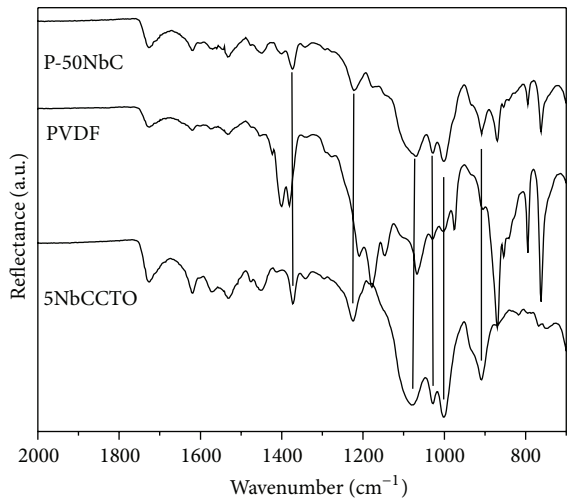

Figure 2: FTIR patterns of NbCCTO, pure PVDF, and P-50NbC.

50 wt% NbCCTO in PVDF matrix have been shown in Figure 1. In case of NbCCTO, the diffraction peaks corresponding to planes (220), (310), (222), (321), (400), (422), and (440) at 2θ values of 34.2°, 38.5°, 42.3°, 45.8°, 49.2°, 61.3°, and 72.2°, respectively, confirmed the formation of single phase compound [20]. There is no evidence of presence of any secondary phase in NbCCTO. Pure PVDF crystallizes in α phase with characteristic 2θ peaks at 17.7°, 18.7°, and 19.9°, corresponding to (110), (020), and (111) crystal planes, respectively [22]. Intensity of three major peaks (220), (400), and (422) of CCTO increases with increasing amount of NbCCTO in the composites. Predominance of NbCCTO phase can be seen in P-50NbC composite due to higher weight percent of ceramic in the composite. It is also the reason for observing suppressed diffraction peaks of PVDF. Average crystallite size determined for P-50NbC composite from broadening of X-ray diffraction peak corresponding to 2θ value of (220) plane using Scherrer's formula has been found to decrease to 47 nm from 59 nm for pure NbCCTO.

Figure 2 shows FTIR spectra of NbCCTO, PVDF, and P-50NbC composite. Peaks of crystalline α PVDF are observed at 763 and 796 cm^{-1} but the peak intensity diminished with reinforcement of NbCCTO. Extra peaks at 908, 1068, 1222, and 1373 cm^{-1} present in the spectrum of composite confirm the presence of NbCCTO in PVDF. Peaks at 1001, 1028, 1532, 1622, and 1725 cm^{-1} become more intense with increasing content of NbCCTO in the composite.

3.2. Surface Morphology. SEM micrographs of pure PVDF, NbCCTO, and composites of P-NbC are shown in Figure 3. It is observed that the spherulitic morphology of pure PVDF gets severely affected by the presence of NbCCTO. Discrete particles of NbCCTO are observed for lower content of the ceramic in the composite (P-10NbC) while aggregation of ceramic particles occurs for higher weight fraction of NbCCTO leading to connected network structure of NbCCTO in P-50NbC composite.

3.3. Mechanical Properties. Samples for mechanical properties were prepared by injection molding technique (Microinjector, Model FD-1, Fly Tech Engineering). Temperature of the mould was maintained at 60°C and that of the cylinder at 210°C under a pressure of 100 bars. Sample prepared by this method had a cross-sectional dimension of (2.15 × 4) mm^2; the length of the gauge section was kept 20 mm. Figure 4 shows the stress-strain curves of PVDF and its composites. Considerable increase was noticed in value of Young's modulus calculated from the slope of the linear region of the plots. For PVDF, P-10NbC, P-20NbC, and P-50NbC, the values are 752, 760, 867, and 1033 MPa, respectively, showing continuous increase with increasing NbCCTO content. This increase in Young's modulus with increase in weight percent of filler can be attributed to interaction between stiffer ceramic and PVDF matrix making composites stiffer as compared to pure PVDF. Elongation at breaking point decreased from 30% in case of PVDF to 20%, 18%, and 16% in case of P-10NbC, P-20NbC, and P-50NbC composites, respectively. The ceramic particles act as defects from a macroscopic point of view and prevent the PVDF chains from packing with each other. This decreases the elongation at breaking point for the composites.

3.4. Dielectric Properties. Frequency dependence of dielectric constant of CCTO and NbCCTO is shown in Figure 5(a). Dielectric constant of CCTO was found to be 3100 at 1 KHz at room temperature. On doping with Nb, there is an increase in the value of dielectric constant which becomes 24,300 at the 1 KHz. Dielectric constant increases with decreasing frequency and vice versa. Increase in dielectric constant with decreasing frequency is due to presence of interfacial polarization which plays an important role in enhancement of dielectric constant in the low frequency region. Interfacial polarization arises due to presence of microheterogeneities in the materials. In case of CCTO, one relaxation is observed in the low frequency range. There seems to be a second

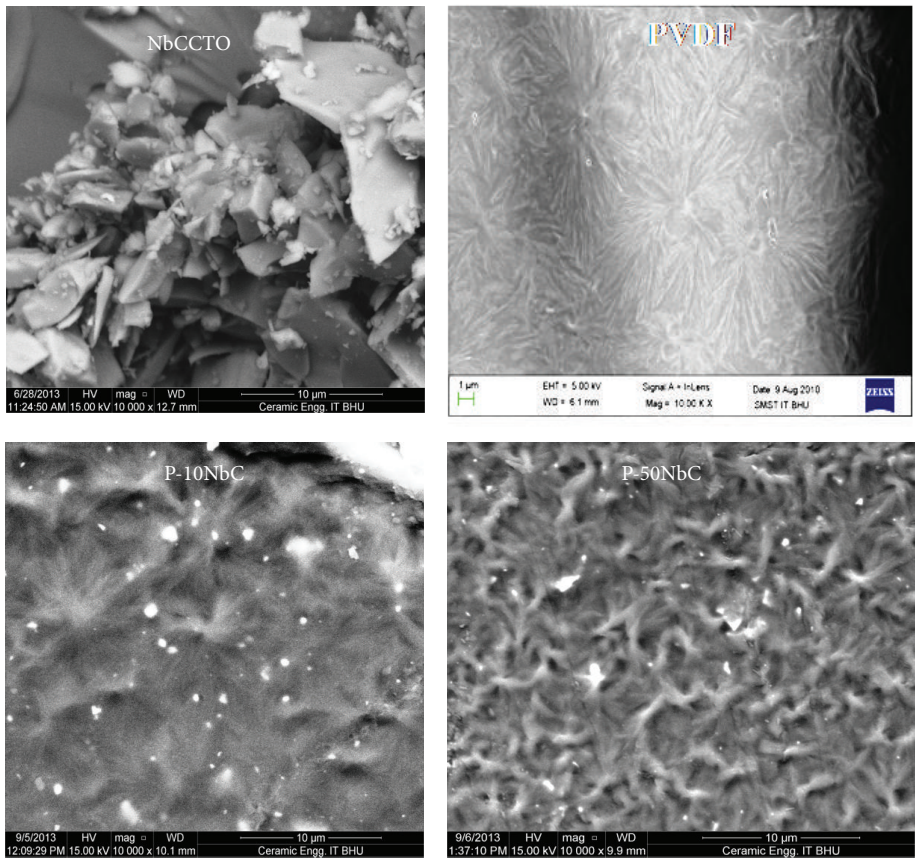

Figure 3: Scanning electron micrographs of NbCCTO, PVDF, P-10NbC, and P-50NbC composite.

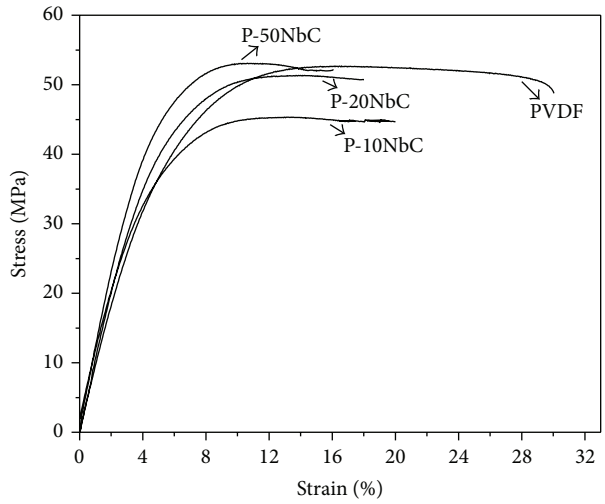

Figure 4: Stress-strain curves for pure PVDF, P-10NbC, P-20NbC, and P-50NbC composites.

relaxation at higher frequency which could not be measured due to limitation of our instrument. In Nb doped CCTO both the relaxations can be seen, one at a frequency around 100 Hz and the other at frequency around 10^5 Hz (Figure 5(b)). It seems that, due to Nb doping, first relaxation observed in CCTO shifts to higher frequency while the second relaxation shifts to lower frequency. With increasing temperature, these relaxations shift towards higher frequency. This indicates lowering of relaxation time (τ) with increasing temperature (Figure 5(b)). Tan δ slightly increases from 0.8 in CCTO to 1.7 in NbCCTO at 100 Hz (Figure 5(b)). Dielectric constant increases with increasing content of NbCCTO in PVDF

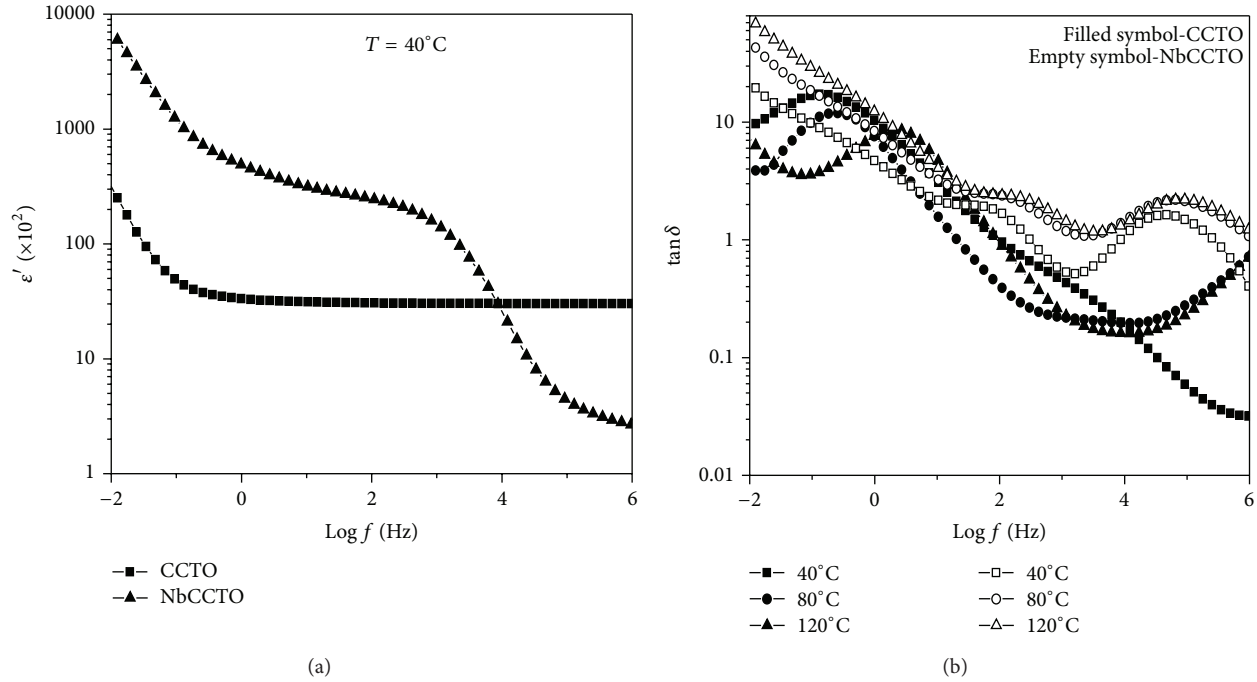

Figure 5: Frequency dependence of effective dielectric constant (a) and tan δ of CCTO and NbCCTO (b).

(Figure 6(a)). Values of dielectric constant at 40°C and 100 Hz for PVDF, P-10NbC P-20NbC, and P-50NbC are 5.2, 20, 29, and 98, respectively. These increase to 7.5, 37, 52, and 148, respectively, at 120°C and 100 Hz. In all the cases, the dielectric constant obtained for composites is much higher than that of pure PVDF. It is important to note that dielectric constant does not change much over the frequency range 10^2–10^6 Hz. It is desirable feature for use in device.

Frequency dependence of tan δ of P-NbC composites is shown in Figure 6. In case of P-NbC composites, one relaxation appears around 10^2–10^4 Hz. The glass transition relaxation of PVDF, denoted by α_a relaxation [26–29], shifts towards much higher frequency which could not be measured due to experimental limitation. Relaxation due to Maxwell Wagner polarization, appearing at slightly less than 100 Hz in NbCCTO, shifts towards higher frequency with the increasing content of NbCCTO in the composites. In case of P-10NbC, this relaxation peak is close to 193 Hz. In case of P-20NbC and P-50NbC, it occurs at 610 Hz and 3200 Hz, respectively. This shift of relaxation peak of NbCCTO to higher frequency in composites indicates lower relaxation time (τ) due to ease of relaxation of dispersed phase in the composite vis-à-vis the condensed phase in ceramic. The relaxation at higher frequency is due to hopping of electrons among Cu^{1+} and Cu^{2+} or among Ti^{3+} and Ti^{4+} or Nb^{4+} and Nb^{5+}. The ceramic samples are produced by sintering at high temperatures. These are expected to lose traces of oxygen during sintering according to the reaction:

$$O_0 \longrightarrow \frac{1}{2}O_2 + V_0^{00} + 2e' \quad (1)$$

where all the species are written in accordance with Kroger Vink notation of defects. Electrons released in the above reaction are captured by Nb^{5+} or Ti^{4+} or Cu^{2+} to produce Nb^{4+} or Ti^{3+}or Cu^{1+}, respectively. Nb^{5+} and Ti^{4+} represent the most stable oxidation state of Nb and Ti, respectively. On the other hand, Cu^{1+} represents the most stable state of Cu having electronic configuration $3d^{10}$. During cooling from sintering temperature, the reverse of the reaction, that is, reoxidation, takes place. But this reoxidation is restricted to grain boundaries and surface only. Therefore these ceramics are expected to contain small concentration of Cu^+ along with Cu^{2+} being in major amount. Electron hopping between Cu^+ and Cu^{2+} is therefore possible. This hopping has activation energies in the range of 0.10–0.20 eV as observed in the present composite samples. Therefore, high frequency relaxation is ascribed to the hopping of electrons among Cu^{1+} and Cu^{2+}. Presence of Cu^{1+}, however, has to be confirmed from XPS study of these samples.

Relaxation time τ was determined using the relation $\tau = 1/2\pi f$ where f is the frequency in cycles per second at the peak position in tanδ versus log$f$ plots. Plots of logτ versus $1000/T$ in the lower and high frequency regions are shown in Figure 7. Values of activation energy obtained from the slopes of these linear plots are given in Table 1. Activation energies for the relaxation at the lower frequency are in the range of 0.20–0.60 eV while these are in the range 0.07–0.20 eV for the higher frequency relaxation. Dielectric relaxation has been studied in the ceramic samples in the system $CaCu_3Ti_4$ $Nb_xO_{12+x/2}$ [25]. Values of activation energies obtained for relaxation at lower frequencies as well as for relaxation at high frequency in these ceramics are close to those obtained in the composites samples in the present study.

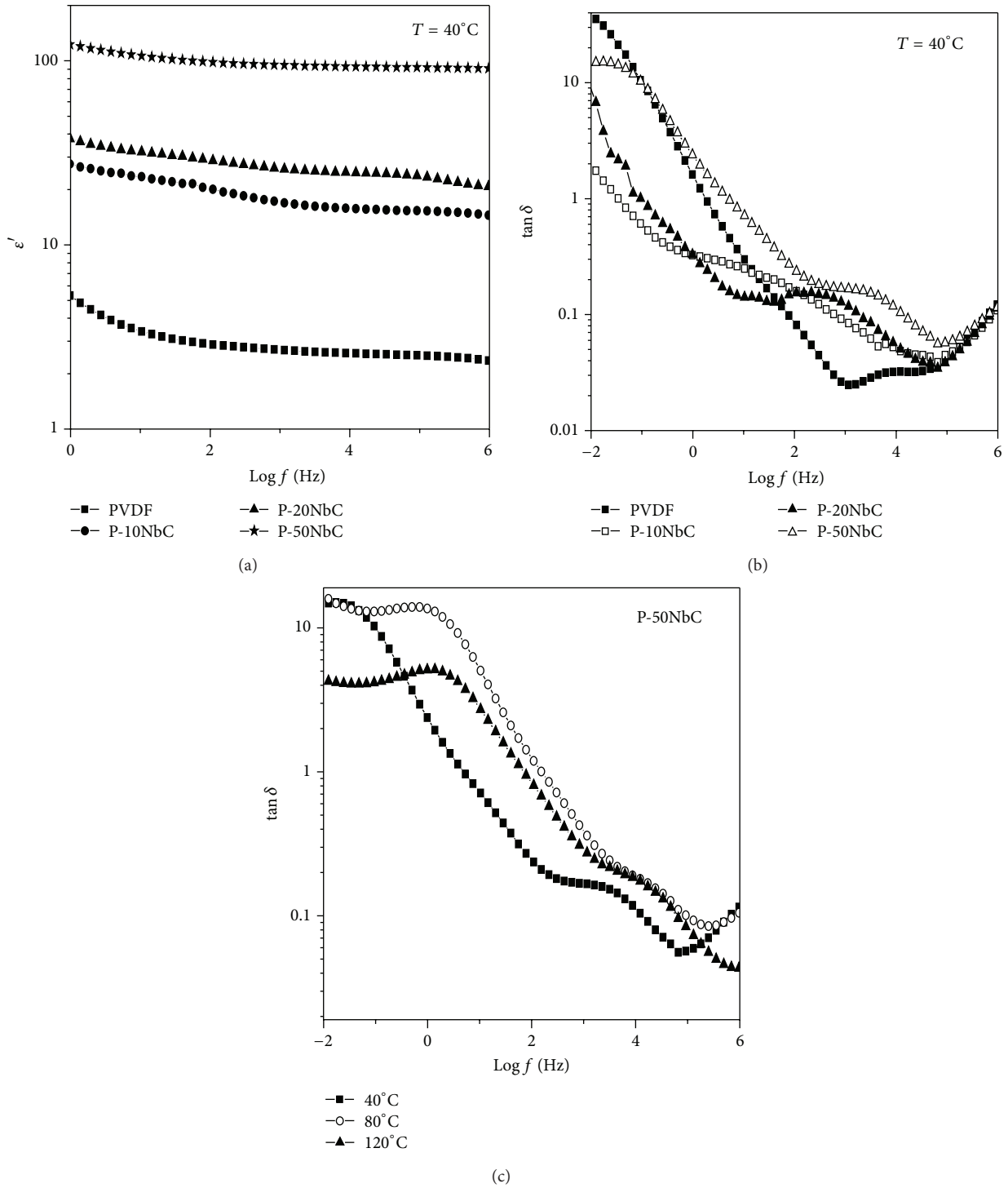

Figure 6: Frequency dependence of effective dielectric constant of PVDF and composites (a), dielectric loss of PVDF and composites at 40°C (b), and tan δ of P-50NbC at different temperature (c).

The temperature-dependent dielectric relaxation is explained by Havriliak-Negami (H-N) function [26, 30]:

$$\varepsilon^* = -i\frac{\sigma_{dc}}{\varepsilon_0 \omega^s} + \varepsilon_\infty + \sum_j \frac{(\Delta\varepsilon)_j}{\left[1 + \left(i\omega\tau_j\right)^\alpha\right]^\beta}, \quad (2)$$

where σ_{dc} is dc conductivity, ω is the angular frequency, s is an exponent ($0 < s \leq 1$), τ_j is the relaxation time of the jth process, ε_0 is the permittivity of vacuum, $\Delta\varepsilon$ is the dielectric strength of the jth process, and α and β are the shape parameters of the H-N function which define the width and the symmetry of the spectrum, respectively. Width parameter α specifies the slope of the lower frequency side of the relaxation peak in ε'' curve and β is the asymmetry parameter and it is calculated using the slope of the relaxation behavior on the higher frequency side of the same curve as

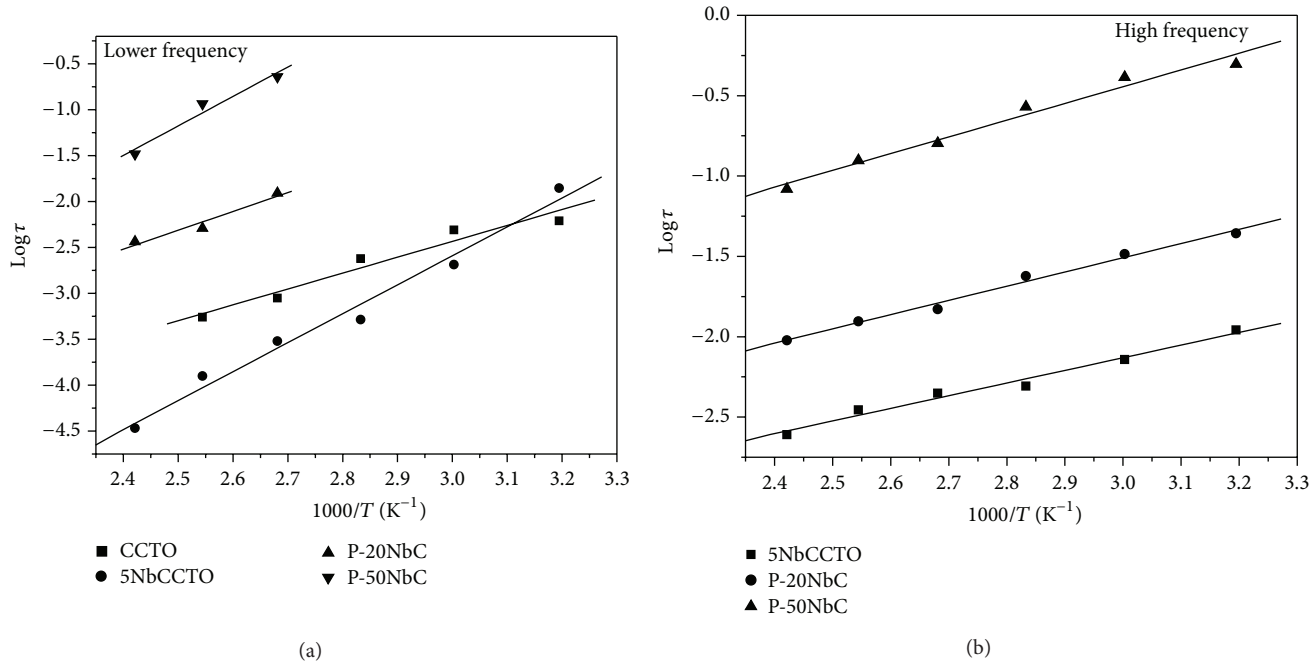

Figure 7: Log τ versus $1000/T$ curves for the low frequency range (a) and high frequency regions (b).

Table 1: Activation energy from tan δ.

	Activation energy from tan δ	
Sample	Low frequency	High frequency
CCTO	0.204 eV	
NbCCTO	0.523 eV	0.102 eV
P-20NbC	0.408 eV	0.17 eV
P-50NbC	0.618 eV	0.20 eV

$\alpha\beta$. Analysis of H-N function using WinFit software program of PVDF and P-50NbC composite has been given in Table 2 using deconvoluted H-N fits presented in Figure 8. In PVDF, β parameter has value of 1 for the temperature range of measurement showing symmetry of the spectrum. But in case of composite, it has different values due to interaction with NbCCTO particles. Relaxation time (s) calculated from H-N fit using WinFit software decreases with increase in temperature for P-50NbC composite. Relaxation time for the composites shows lower value as compared to pure PVDF. Less value of relaxation time at higher temperature is explained on the basis of ease of relaxation at higher temperature due to increased mobility of chains for both pure PVDF and its composites. On the other hand, at a particular temperature, the relaxation time decreases in the composites vis-à-vis pure PVDF mainly because of relaxation facilitation of tiny particles of ceramic dispersed in polymer matrix as compared to larger associated grains in condensed ceramics. The exponent parameter, α, describes different spectral shapes. The higher value of α for composites as compared to pure PVDF indicates a stretched relaxation over a wider range of frequencies than the Debye relaxation usually observed in pure polymer with $\beta = 1$. It can be seen from Figure 8 that in case of P-50NbC composite the relaxation peak shifts towards higher frequency.

4. Conclusion

$CaCu_3Ti_4O_{12}$ and Nb doped $CaCu_3Ti_4O_{12}$ (NbCCTO) have been synthesised by solid state conventional technique. Composites of PVDF and NbCCTO (P-NbC) have been prepared by melt extrusion process. XRD studies indicate no structural change in either polymer or ceramic in the composite but the change in d-spacing indicates better interaction between PVDF and NbCCTO. It is found that Young's modulus increases in the composites. There is a substantial increase in the dielectric constant of CCTO with Nb doping accompanied by a slight increase in dielectric loss. Addition of NbCCTO in PVDF increases the dielectric constant significantly. In composites, dielectric loss is slightly more than that in pure PVDF. The relaxation peaks shift towards higher frequencies in the composites suggesting lowering of relaxation time. This is mainly because of the easiness of relaxation in tiny ceramic particles well dispersed in composites as opposed to that in stiffer condensed ceramic phase. The potential application of these materials can be in the form of embedded capacitors. The challenges associated with implementation of this technology are related to the enhancement of dielectric constant and reduction of dielectric loss. Temperature dependence of dielectric relaxation has been worked out in detail through H-N function. Debye type relaxation is observed in pure PVDF with $\beta = 1$. Stretched

Table 2: Fitting parameters for α_c relaxation as a function of temperature obtained from H-N fits.

Temp.	PVDF, α	P-50NbC, α	PVDF, β	P-50NbC, β	PVDF, τ	P-50NbC, τ
40	0.49	0.62	1	0.59	$2.33E-2$	$4.32E-2$
80	0.53	0.65	1	0.61	$1.45E-3$	$6.26E-3$
120	0.57	0.76	1	0.71	$7.44E-4$	$2.18E-5$

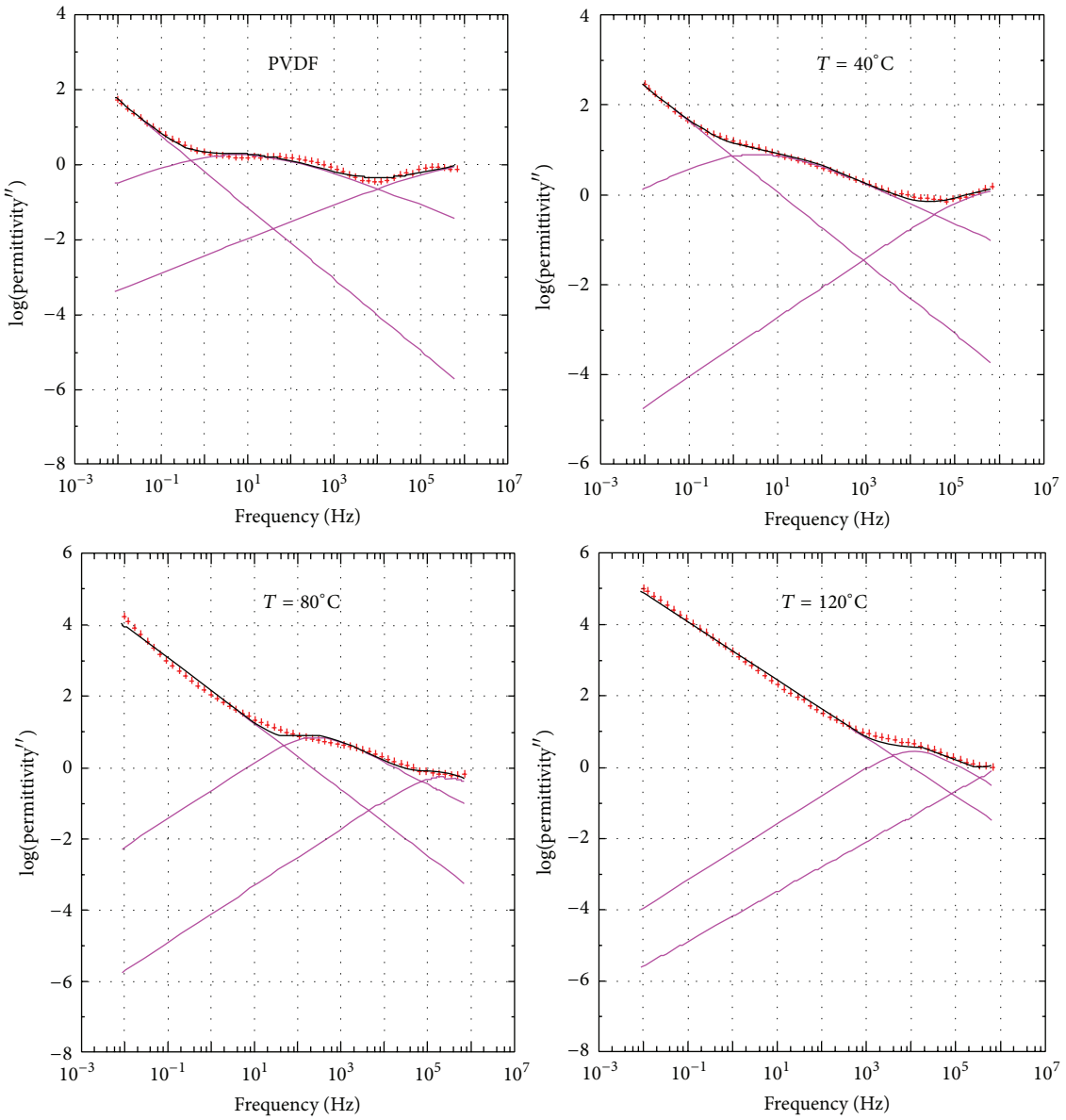

Figure 8: Dielectric loss in the frequency domain and spectrum was deconvoluted from H-N fits for P-50NbC.

relaxation has been observed over a wider range of frequency in the composite suggesting asymmetric nature of relaxation.

Conflict of Interests

The authors declare that there is no conflict of interests regarding the publication of this paper.

References

[1] R. R. Tummala, *Electronic Packaging for High Reliability, Low Cost Electronics*, Kluwer Academic, 1999.

[2] J. Lau, *Chip on Board Technologies for Multichip Modules*, Kluwer Academic, 1994.

[3] E. H. Immergut, J. Brandrup, and W. McDowell, *Polymer Handbook*, Wiley, New York, NY, USA, 2008.

[4] R. E. Newnham, "Composite electroceramics," *Annual Review of Materials Science*, vol. 16, pp. 47–68, 1986.

[5] D. K. Das-Gupta and K. Doughty, "Polymer-ceramic composite materials with high dielectric constants," *Thin Solid Films*, vol. 158, no. 1, pp. 93–105, 1988.

[6] D. K. Das-Gupta, *Key Engineering Materials*, Trans Tech Publications, 1994.

[7] Y. Bai, Z.-Y. Cheng, V. Bharti, H. S. Xu, and Q. M. Zhang, "High-dielectric-constant ceramic-powder polymer composites," *Applied Physics Letters*, vol. 76, no. 25, pp. 3804–3806, 2000.

[8] S. U. Adikary, H. L. W. Chan, C. L. Choy, B. Sundaravel, and I. H. Wilson, "Characterisation of proton irradiated $Ba_{0.65}Sr_{0.35}TiO_3$/P(VDF-TrFE) ceramic-polymer composites," *Composites Science and Technology*, vol. 62, no. 16, pp. 2161–2167, 2002.

[9] Z.-M. Dang, Y.-F. Yu, H.-P. Xu, and J. Bai, "Study on microstructure and dielectric property of the $BaTiO_3$/epoxy resin composites," *Composites Science and Technology*, vol. 68, no. 1, pp. 171–177, 2008.

[10] Z. H. Dang, Y. Q. Lin, H. P. Xu, C. Y. Shi, S. H. Li, and J. B. Bai, "Fabrication and dielectric characterization of advanced $BaTiO_3$/polyimide nanocomposite films with high thermal stability," *Advanced Functional Materials*, vol. 18, no. 10, pp. 1509–1517, 2008.

[11] C. Muralidhar and P. K. C. Pillai, "Dielectric behaviour of barium titanate-polyvinylidene fluoride composites," *Journal of Materials Science*, vol. 23, no. 3, pp. 1071–1076, 1988.

[12] Z.-M. Dang, Y. Shen, and C.-W. Nan, "Dielectric behavior of three-phase percolative Ni-$BaTiO_3$/polyvinylidene fluoride composites," *Applied Physics Letters*, vol. 81, no. 25, pp. 4814–4816, 2002.

[13] M. A. Subramanian, D. Li, N. Duan et al., "High dielectric constant in a $ACu_3Ti_4O_{12}$ and $ACu_3Ti_3FeO_{12}$ phases," *Journal of Solid State Chemistry*, vol. 151, pp. 323–325, 2000.

[14] W. Yang, S. Yu, R. Sun, and R. Du, "Nano- and microsize effect of CCTO fillers on the dielectric behavior of CCTO/PVDF composites," *Acta Materialia*, vol. 59, no. 14, pp. 5593–5602, 2011.

[15] B. Chu, X. Zhou, K. Ren, B. Neese, M. Lin, and Q. Zhang, "A dielectric polymer with high electric energy density and fast discharge peed," *Science*, vol. 313, no. 5785, pp. 334–337, 2006.

[16] J. Y. Li, L. Zhang, and S. Ducharme, "Electric energy density of dielectric composites," *Applied Physics Letters*, vol. 90, Article ID 132901, 2007.

[17] M. Arbatti, X. Shan, and Z. Cheng, "Ceramic-polymer composites with high dielectric constant," *Advanced Materials*, vol. 19, no. 10, pp. 1369–1372, 2007.

[18] C. Yang, H. S. Song, and D. B. Liu, "Effect of coupling agents on the dielectric properties of $CaCu_3Ti_4O_{12}$/PVDF composites," *Composite: Part B*, vol. 50, pp. 180–186, 2013.

[19] L. Zhang, X. Shan, P. Wu, and Z.-Y. Cheng, "Dielectric characteristics of $CaCu_3Ti_4O_{12}$/P(VDF-TrFE) nanocomposites," *Applied Physics A*, vol. 107, no. 3, pp. 597–602, 2012.

[20] P. Thomas, S. Satapathy, K. Dwarakanath, and K. B. R. Varma, "Dielectric properties of poly(vinylidene fluoride)/$CaCu_3Ti_4O_{12}$ nanocrystal composite thick films," *EXPRESS Polymer Letters*, vol. 4, no. 10, pp. 632–643, 2010.

[21] Z. M. Dang, T. Zhou, S. H. Yao et al., "Advanced calcium copper titanate/polyimide functional hybrid films with high dielectric permittivity," *Advanced Materials*, vol. 21, no. 20, pp. 2077–2082, 2009.

[22] P. Thomas, K. T. Varughese, K. Dwarakanath, and K. B. R. Varma, "Dielectric properties of poly(vinylidene fluoride)/$CaCu_3Ti_4O_{12}$ composites," *Composite Science and Technology*, vol. 70, pp. 539–545, 2010.

[23] D. C. Sinclair, T. B. Adams, F. D. Morrison, and A. R. West, "$CaCu_3Ti_4O_{12}$: one-step internal barrier layer capacitor," *Applied Physics Letters*, vol. 80, no. 12, pp. 2153–2155, 2002.

[24] M. A. Sulaiman, S. D. Hutagalung, M. F. Ain, and Z. A. Ahmad, "Dielectric properties of Nb-doped $CaCu_3Ti_4O_{12}$ electroceramics measured at high frequencies," *Journal of Alloys and Compounds*, vol. 493, no. 1-2, pp. 486–492, 2010.

[25] S.-H. Hong, D.-Y. Kim, H.-M. Park, and Y.-M. Kim, "Electric and dielectric properties of Nb-doped $CaCu_3Ti_4O_{12}$ ceramics," *Journal of the American Ceramic Society*, vol. 90, no. 7, pp. 2118–2121, 2007.

[26] H. Windlass, P. M. Raj, D. Balaraman, S. K. Bhattacharya, and R. R. Tummala, "Colloidal processing of polymer ceramic nanocomposites for integral capacitors," in *Proceedings of the IEEE International Symposium on Advanced Packaging Materials: Processes, Properties and Interfaces*, pp. 393–398, Braselton, Ga, USA, March 2001.

[27] R. Gregorio Jr. and M. Cestari, "Effect of crystallization temperature on the crystalline phase content and morphology of poly(vinylidene fluoride)," *Journal of Polymer Science Part B: Polymer Physics*, vol. 32, no. 5, pp. 859–870, 1994.

[28] R. Gregorio Jr. and E. M. Ueno, "Effect of crystalline phase, orientation and temperature on the dielectric properties of poly (vinylidene fluoride) (PVDF)," *Journal of Materials Science*, vol. 34, no. 18, pp. 4489–4500, 1999.

[29] C. V. Chanmal and J. P. Jog, "Dielectric relaxations in PVDF/$BaTiO_3$ nanocomposites," *Express Polymer Letters*, vol. 2, no. 4, pp. 294–301, 2008.

[30] J. Mijović, H. Lee, J. Kenny, and J. Mays, "Dynamics in polymer-silicate nanocomposites as studied by dielectric relaxation spectroscopy and dynamic mechanical spectroscopy," *Macromolecules*, vol. 39, no. 6, pp. 2172–2182, 2006.